Preparation of a SiO_2-covered amorphous CoFeSiB microwire and study on the current amplitude effect on the transverse giant magnetoimpedance

Tao Wang[1] ✉, *Yi He*[1], *Yuyi Chen*[1], *Dongya Huang*[2], *Jun Yang*[2], *Jinjun Rao*[1], *Hengyu Li*[1], *Bicong Wang*[1], *Bowen Wang*[3], *Mei Liu*[1]

[1]*School of Mechatronics Engineering and Automation, Shanghai University, Shanghai 200444, People's Republic of China*
[2]*Luoyang Ship Materials Research Institute, Luoyang 471023, People's Republic of China*
[3]*China Coal Technology Engineering Group Chongqing Research Institute, Chongqing 400039, People's Republic of China*
✉ *E-mail: wangt@shu.edu.cn*

Published in Micro & Nano Letters; Received on 10th September 2018; Revised on 10th December 2018; Accepted on 21st December 2018

A SiO_2-covered amorphous wire was prepared by the melt spinning technique for investigation of the current amplitude effect on the giant magnetoimpedance (GMI). The raw alloy (CoFeSiB) was placed in a SiO_2 tube and heated by induced current (600 A) for 50 s, then the SiO_2-covered amorphous wire was formed through external traction and cooling water. The current amplitude effects on the transverse GMI, giant magnetoresistance (GMR) and giant magnetoreactance (GMX) in the SiO_2-covered amorphous CoFeSiB wire were studied thoroughly. It was observed that the transverse GMI ratio, GMR ratio, and GMX ratio all increase with decreasing the current amplitude, demonstrating the possibility of using them to design low-consumption, high-sensitive and muti-dimension magnetometer.

1. Introduction: Amorphous soft magnetic alloys are very useful for the development of high-performance magnetic sensors due to its excellent soft magnetic property including high magnetisation saturation intensity, low magnetic hysteresis, and low coercivity. Compared with those of the conventional magnetic sensors [1–4], the giant magnetoimpedance (GMI) sensors based on soft magnetic microwires indeed owe higher field-sensitivity, the alternating current (AC) impedance of which can reach a sensitivity of 600% in the microwires [5–16], which is especially suited for fabrication of highly sensitive GMI sensors.

In recent years, much attention is paid to the investigation of the longitudinal GMI effect, while the GMI sensors based on the longitudinal GMI effect cannot be used to determine the magnetic field direction due to its symmetrical structure. There has been relatively little research on the transverse GMI effect [17, 18] in recent years. Study of the transverse GMI effect gives helpful information to develop a multi-dimension magnetometer for determination of the magnetic field direction. Until now, the studies on the influences of the current amplitude on the transverse GMI effect in the soft amorphous wires are scarcely reported. In this work, we focus on the study of the current amplitude effect on the transverse GMI effect, giant magnetoresistance (GMR) effect and giant magnetoreactance (GMX) effect in a SiO_2-covered amorphous CoFeSiB wire in order to develop a highly sensitive low-consumption magnetometer.

2. Experiment: Since the glass-covered microwire exhibits excellent good ductility, excellent flexibility and strong GMI effect [7, 8], a SiO_2-covered amorphous CoFeSiB microwire was tested in this work. The GMI sensor (CoFeSiB microwire) was obtained from our cooperative partner (Luoyang Ship Material Research Institute) with the length and diameter of 2 cm and 66.94 µm, respectively.

A SiO_2-covered amorphous CoFeSiB microwire used in this study was prepared by the melt spinning method. The raw material (CoFeSiB) was placed in a SiO_2 tube, and the SiO_2 tube was entirely placed in a high-frequency induction coil, then the alloy was heated by the induced current (portable electric induction heating machine, the heating current is 600 A) for 50 s. The melted alloy and SiO_2 formed a micro-melting pool together with the softened SiO_2 tube wall, then the external end of the microfilament was drawn out into a micron-sized SiO_2-covered amorphous wire, as shown in Fig. 1*a*. As can be seen from Fig. 1*b*, the total thickness (diameter) of the wire is 66.94 µm, the thicknesses of the SiO_2 and COFeSiB are about 4.24 and 29.23 µm, respectively. The energy dispersive X-ray analysis (EDX) results in Table 1 confirm that Si and O elements take up the major slice of the sample, almost reaches %. The EDX results in Table 2 confirm that the core of the wire is composed of CoFeSiB alloy.

During the test, the microwire was immobilised on a plane, both of its ends were connected to the Impedance analyser E4990A with an AC current flowing through the wire in different frequencies (20 Hz–15 MHz) and different current amplitudes (1–5 mA). An external magnetic field (0–100 Oe) produced by a solenoid coil was applied transversely on the wire.

In this work, the impedance variation, resistance variation, and reactance variation were characterised by the relative change in impedance (GMI ratio), resistance (GMR ratio) and reactance (GMX ratio), respectively, which were defined as

$$\text{GMI ratio} = \Delta Z/Z = 100\% \times \frac{Z(H) - Z(H_{\max})}{Z(H_{\max})}, \quad (1)$$

$$\text{GMR ratio} = \Delta R/R = 100\% \times \frac{R(H) - R(H_{\max})}{R(H_{\max})}, \quad (2)$$

$$\text{GMX ratio} = \Delta X/X = 100\% \times \frac{X(H) - X(H_{\max})}{X(H_{\max})}, \quad (3)$$

where $Z(H)$, $R(H)$, and $X(H)$ represent the impedance, resistance, and reactance under an external magnetic field (H), where $Z(H_{\max})$, $R(H_{\max})$, and $X(H_{\max})$ represent the impedance, resistance, and reactance under the maximum external magnetic field ($H_{\max}$), respectively. The GMI ratio, GMR ratio, and GMX ratio were measured under different conditions, respectively.

3. Result and discussion: As can be seen in Fig. 2, all the curves show that the GMI ratio increases firstly and decreases with the increasing external magnetic field, the maximum GMI ratios of all the curves are obtained nearly at $H = 1$ Oe. This is due to the fact that the quasi-free magnetisation responds quickly to the

doi: 10.1049/mnl.2018.5547

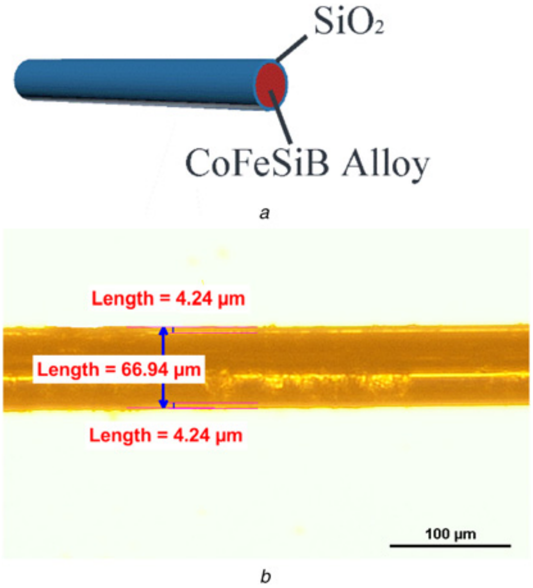

Fig. 1 *The SiO_2-covered amorphous CoFeSiB microwire*
a SiO_2-covered amorphous CoFeSiB microwire sketch
b Microscopy image of the SiO_2-covered amorphous CoFeSiB microwire

Table 1 EDX analysis of the SiO_2 layer

Elt.	Line	Intensity, c/s	Conc.	Units
O	Ka	630.88	55.882	wt.%
Na	Ka	80.41	4.238	wt.%
Al	Ka	60.54	2.465	wt.%
Si	Ka	929.99	37.416	wt.%
			100.000	total

Table 2 EDX analysis of the CoFeSiB core

Elt.	Line	Intensity, c/s	Conc.	Units
B	Ka	17.95	0.719	wt.%
Si	Ka	249.09	8.793	wt.%
Fe	Ka	45.36	4.771	wt.%
Co	Ka	599.12	85.717	wt.%
			100.000	total

external oscillating magnetic field and the magnetic permeability of the wire is improved significantly at the switching field (<5 Oe) [19–21]. Thus, the GMI ratio reaches the first maximal value at the switching field. The magnetic field dependence curve (Fig. 2) shows the typical transverse GMI property, the GMI ratio starts to decrease from an almost zero field, which exhibits a different tendency compared with the longitudinal GMI curve. It can be explained by the similar theory: for a transverse annealing wire with a small AC current, the maximum circular magnetic permittivity is obtained at zero-transverse external magnetic field [18, 22, 23]. The domain wall movement is inhibited by the presence of the transverse magnetic field. Hence, the maximum GMI ratio is obtained at zero fields, and the circular magnetic permittivity gradually decreases along with increasing the transverse magnetic field [20–23].

The GMI ratios seem to be disordered at a low external magnetic field (< 3 Oe), which is due to the fact that the soft magnetic wire exhibits slight magnetic hysteresis at a low-magnetic field. After that the GMI ratio decreases with increasing current amplitude at a high external magnetic field, then the GMI ratios gradually

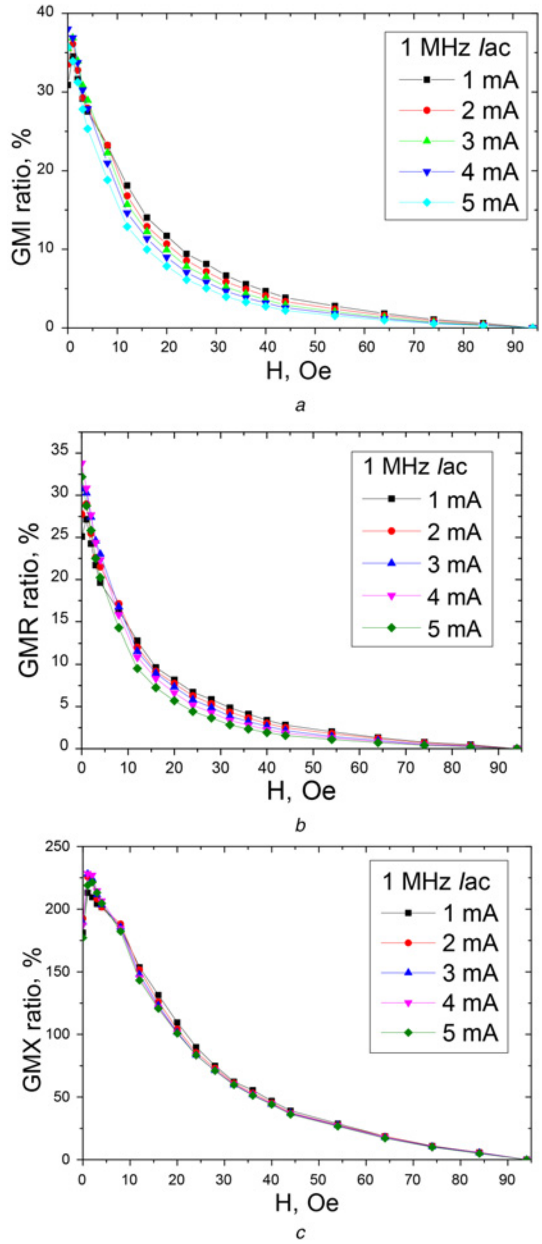

Fig. 2 *GMI ratio tendency curves with the external magnetic field*
a GMI ratio
b GMR ratio
c GMX ratio

become stable and independent of the current amplitude as the external magnetic field is further increased. Actually, the transverse and longitudinal GMI effect can be attributed to the changes of the longitudinal permeability and transverse permeability [24, 25]. The change in impedance is directly related to the circular magnetisation process [22, 23] induced by the AC current. At higher transverse external magnetic field (>10 Oe), increasing current amplitude may inhibit the transverse magnetisation process, which could lead to a decreasing of the longitudinal permeability and thus the transverse GMI effect.

The GMI curves of frequency dependency are shown in Fig. 3. Apparently, the GMI tendency of *Z* is similar to that of *R*, all the GMI curves show a similar tendency that the GMI ratios increase firstly and then decrease with increasing the frequency. This is because the skin effect of the high-frequency current is the origin of the GMI effect, which has greatly modified the impedance at 2 MHz [20–23]. Hence, the GMI ratio increases with increasing

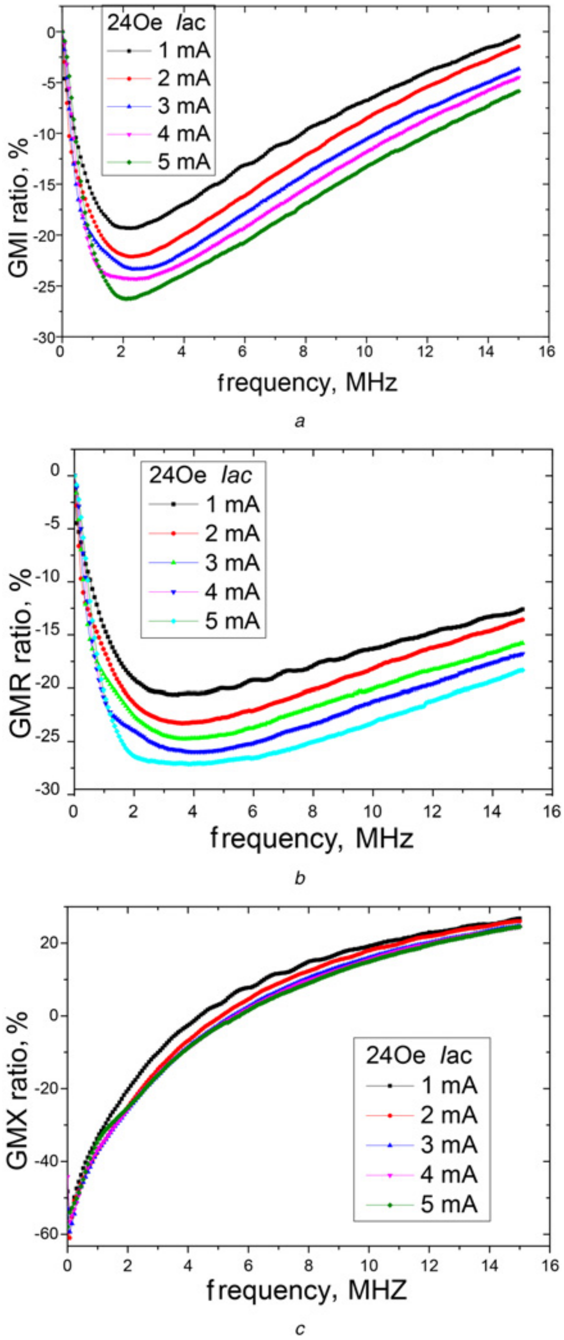

Fig. 3 *GMI ratio tendency curves with the frequency dependency*
a GMI ratio
b GMR ratio%
c GMX ratio

the frequency from 20 Hz to 2 MHz. After that, the GMI ratio decreases gradually, seeming to be different from the longitudinal GMI effect in the soft magnetic wires, the maximal value of which is obtained at over 10 MHz. This is due to the fact that the longitudinal permeability is much smaller than the annular permeability for a wire, thus, the GMI ratio of the transverse GMI effect always reaches the maximal value at a relatively lower frequency compared with the longitudinal GMI effect [22]. Anyway, the results provide useful information for the design of a low-frequency sensor based on the transverse GMI effect. The GMI curve of the *X* shows a different trend that the GMI ratios of different curves all increase with increase in the frequency. It can be easily explained by that the GMI effect is mainly caused by the magnetoinductive

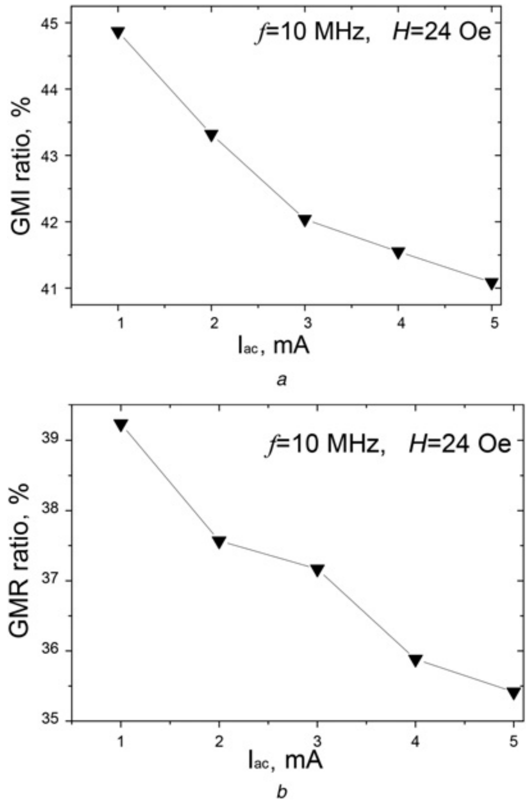

Fig. 4 *GMI ratio and GMR ratio change with the current amplitude at f = 10 MHz and H = 24 Oe*
a GMI ratio
b GMR ratio

effect at low frequency (KHz), *X* reaches the maximal value at several KHz, then it decreases with increasing frequency [19, 20, 22, 23]. The inductance is the main contribution to the GMI effect at low frequency, while the resistance contributes to the GMI effect at a higher frequency. As shown in Fig. 4, the GMI ratio decreases with increasing the AC amplitude. This is because the increasing of current amplitude may inhibit the transverse magnetisation process, modifying the longitudinal permeability and thus the transverse GMI effect.

It is obvious from Fig. 4, the GMR ratio and the GMI ratio both decrease with increasing the current amplitude. The GMI ratio even can reach a large variation of 45% at a small current amplitude of 1 mA at $f = 10$ MHz and $H = 24$ Oe. Therefore, the transverse GMI effect in the microwire is very useful for the development of a highly sensitive low-consumption magnetoimpedance sensor.

4. Conclusion: In this work, we have thoroughly studied the current amplitude effect on the transverse GMI, GMR, and GMX. The results indicate that the GMI ratio, GMR ratio and GMX ratio all decrease with increasing AC amplitude, which provides useful information for the design of the low-consumption magnetic sensor. A strong transverse magnetoreactance effect can be obtained at a low frequency compared with the longitudinal GMI effect, which may explore a new pathway for development of a high-sensitive, low-frequency and multi-dimension magnetometer for the detection of weak magnetic fields.

5. Acknowledgments: This work is supported by the National Youth Natural Science Foundation (grant no. 61703266), the National Natural Science Foundation of China (grant no. 51675321), the National Science Fund for Distinguished Young Scholars (grant no. 61525305), the National Science Fund for Distinguished Young Scholars (grant no. 61625304), the Natural

doi: 10.1049/mnl.2018.5547

Science Foundation of Shanghai (grant no. 17ZR1409700), the Natural Science Foundation of Shanghai (grant no. 18ZR1415300), the National Natural Science Foundation of China (grant no. 61573236).

6 References

[1] Besse P., Boero G., Demierre M., ET AL.: 'Detection of a single magnetic microbead using a miniaturized silicon hall sensor', *Appl. Phys. Lett.*, 2002, **80**, (22), pp. 4199–4201

[2] Rifai D., Abdalla A., Ali K., ET AL.: 'Giant magnetoresistance sensors: a review on structures and non-destructive eddy current testing applications', *Sensors*, 2016, **16**, (3), p. 298

[3] Jiang F., Liu S.: 'Evaluation of cracks with different hidden depths and shapes using surface magnetic field measurements based on semi-analytical modelling', *J. Phys. D, Appl. Phys.*, 2018, **51**, (12), p. 125002

[4] Ziegler S., Woodward R.C., Iu H.H., ET AL.: 'Current sensing techniques: a review', *IEEE Sens. J.*, 2009, **9**, (4), pp. 354–376

[5] Mishra A.C., Sahoo T., Srinivas V., ET AL.: 'Giant magnetoimpedance in electrodeposited CoNiFe/Cu wire: a study on thickness dependence', *J. Alloys Compd.*, 2009, **480**, (2), pp. 771–776

[6] Ning N., Fan J., Wu J., ET AL.: 'NiFe/insulator/Cu composite wires and their giant magneto-impedance effects', *Surf. Rev. Lett.*, 2010, **17**, (3), pp. 369–373

[7] Beck F., Gomes R.C., Sossmeier K.D., ET AL.: 'Stress dependence of the domain wall dynamics in the adiabatic regime', *J. Magn. Magn. Mater.*, 2011, **323**, (3–4), pp. 268–271

[8] Chiriac H.: 'Preparation and characterization of glass covered magnetic wires', *Mater. Sci. Eng. A*, 2001, **304**, pp. 166–171

[9] García-Chocano V.M., García-Miquel H.: 'DC and AC linear magnetic field sensor based on glass coated amorphous microwires with giant magnetoimpedance', *J. Magn. Magn. Mater.*, 2015, **378**, pp. 485–492

[10] Ipatov M., Zhukova V., Gonzalez J., ET AL.: 'Manipulating the magnetoimpedance by dc bias current in amorphous microwire', *J. Magn. Magn. Mater.*, 2012, **324**, (23), pp. 4078–4083

[11] Chen D.L., Li X., Pan H.L., ET AL.: 'Magneto-impedance effect of composite wires prepared by chemical plating under DC current', *Nano-Micro Lett.*, 2014, **6**, (3), pp. 227–232

[12] Chiriac H., Ovari T.A.: 'Novel trends in the study of magnetically soft Co-based amorphous glass-coated wires', *J. Magn. Magn. Mater.*, 2011, **323**, (23), pp. 2929–2940

[13] Sun J.F., Liu J.S., Xing D.W., ET AL.: 'Experimental study on the effect of alternating-current amplitude on GMI output stability of Co-based amorphous wires', *Phys. Status Solidi A*, 2011, **208**, (4), pp. 910–914

[14] Kurlyandskaya G.V., Bebenin N.G., Vas'Kovsky V.O.: 'Giant magnetic impedance of wires with a thin magnetic coating', *Phys. Metals Metallogr.*, 2011, **111**, (2), pp. 133–154

[15] Rao K.V., Humphrey F.B., Costa-Kramer J.L.: 'Very large magneto-impedance in amorphous soft ferromagnetic wires (invited)', *J. Appl. Phys.*, 1994, **76**, (10), pp. 6204–6208

[16] Zhukova V., Chizhik A., Zhukov A., ET AL.: 'Optimization of giant magnetoimpedance in Co-rich amorphous microwires', *IEEE Trans. Magn.*, 2002, **38**, (5), pp. 3090–3092

[17] Wang Z.C., Gong F.F., Yang X.L., ET AL.: 'Longitudinally driven giant magnetoimpedance effect in stress-annealed Fe-based nanocrystalline ribbons', *J. Appl. Phys.*, 2000, **87**, (9), pp. 4819–4821

[18] Zhou Z.Z., Zhou Y., Chen L., ET AL.: 'Transverse, longitudinal and perpendicular giant magnetoimpedance effects in a compact multiturn meander NiFe/Cu/NiFe trilayer film sensor', *Meas. Sci. Technol.*, 2011, **22**, (3), p. 035202

[19] Mohri K., Kohzawa T., Kawashima K., ET AL.: 'Magneto-inductive effect (MI effect) in amorphous wires', *IEEE Trans. Magn.*, 1992, **28**, (5), pp. 3150–3152

[20] Panina L.V., Mohri K.: 'Magnetoimpedance effect in amorphous wires', *Appl. Phys. Lett.*, 1994, **65**, (9), pp. 1189–1191

[21] Vázquez M.: 'Giant magneto-impedance in soft magnetic 'wires'', *J. Magn. Magn. Mater.*, 2001, **226**, pp. 693–699

[22] Knobel M., Pirota K.R.: 'Giant magnetoimpedance: concepts and recent progress', *J. Magn. Magn. Mater.*, 2002, **242**, pp. 33–40

[23] Phan M.H., Peng H.X.: 'Giant magnetoimpedance materials: fundamentals and applications', *Prog. Mater. Sci.*, 2008, **53**, pp. 323–420

[24] Sommer R.L., Chien C.L.: 'Longitudinal, transverse, and perpendicular magnetoimpedance in nearly zero magnetostrictive amorphous alloys', *Phys. Rev. B*, 1995, **53**, (10), p. R5982

[25] Sommer R.L., Chien C.L.: 'Longitudinal and transverse magneto-impedance in amorphous $Fe_{73.5}Cu_1Nb_3Si_{13.5}B_9$ films', *Appl. Phys. Lett.*, 1995, **67**, (22), p. 3346